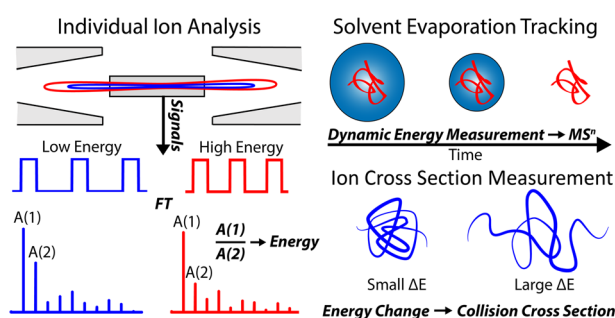


Determining Energies and Cross Sections of Individual Ions Using Higher-Order Harmonics in Fourier Transform Charge Detection Mass Spectrometry (FT-CDMS)

Conner C. Harper, Andrew G. Elliott, Haw-Wei Lin, Evan R. Williams

Department of Chemistry, University of California, Berkeley, CA 94720-1460, USA



Abstract. A general method for in situ measurements of the energy of individual ions trapped and weighed using charge detection mass spectrometry (CDMS) is described. Highly charged ($> 300 e$), individual polyethylene glycol (PEG) ions are trapped and oscillate within an electrostatic trap, producing a time domain signal. A segmented Fourier transform (FT) of this signal yields the temporal evolution of the fundamental and harmonic frequencies of ion motion throughout the 500-ms trap time.

The ratio of the fundamental frequency and second harmonic (HAR) depends on the ion energy, which is an essential parameter for measuring ion mass in CDMS. This relationship is calibrated using simulated ion signals, and the calibration is compared to the HAR values measured for PEG ion signals where the ion energy was also determined using an independent method that requires that the ions be highly charged ($> 300 e$). The mean error of 0.6% between the two measurements indicates that the HAR method is an accurate means of ion energy determination that does not depend on ion size or charge. The HAR is determined dynamically over the entire trapping period, making it possible to observe the change in ion energy that takes place as solvent evaporates from the ion and collisions with background gas occur. This method makes it possible to measure mass changes, either from solvent evaporation or from molecular fragmentation (MS^n), as well as the cross sections of ions measured using CDMS.

Keywords: Charge detection mass spectrometry, Ion mobility, Ion energy, Megadalton, Collision cross section, MS^n , Harmonics, Fourier transform

Received: 24 March 2018/Revised: 26 April 2018/Accepted: 3 May 2018/Published Online: 2 June 2018

Introduction

Multiple charged ions of a wide variety of polymers and noncovalent complexes can be formed directly from solution with electrospray ionization (ESI). In conventional mass spectrometry (MS) measurements, the mass-to-charge ratios (m/z) of ensembles of ions are measured and information about the charge states is obtained from the spacings of isotopic peaks or from spacings in the charge-state distributions of ions

of the same mass. Charge-state distributions have been resolved for purified molecular complexes up to ~ 20 MDa in size [1]. However, sample heterogeneity and adduction often limit the ability to resolve charge states, making mass measurements difficult or impossible even for much smaller molecules [2]. An alternative to conventional MS techniques that eliminates the problem of sample heterogeneity is to simultaneously measure both the m/z and charge of individual ions. Single ion techniques have been implemented in Fourier transform ion cyclotron resonance [3, 4] and quadrupole ion trap [5–10] instruments to measure the masses of large (MDa) ions. However, these techniques have not gained widespread use due to the long times required for each ion measurement.

Charge detection mass spectrometry (CDMS) has undergone significant recent developments that make it an excellent

Electronic supplementary material The online version of this article (<https://doi.org/10.1007/s13361-018-1987-x>) contains supplementary material, which is available to authorized users.

Correspondence to: Evan Williams; e-mail: erw@berkeley.edu

choice for measuring masses of large molecules in complex mixtures that are not readily amenable to analysis with more conventional methods. In CDMS, an ion is passed through a conductive cylinder resulting in an induced charge pulse in the detection circuit that has an amplitude which is proportional to the charge of the ion. The m/z of an ion with a known kinetic energy is determined from its measured velocity. CDMS instruments in which the ion passes once through a single detector tube have been used to measure the mass and charge of cosmic dust [11–13], synthetic polymers [14], viruses [15], DNA [16, 17], and nanoparticles [18, 19]. However, the uncertainty in the measured charge using a single-pass instrument is high ($> 75 e$), leading to correspondingly large uncertainties in mass measurement [15]. To increase the signal-to-noise ratios of these measurements and improve the accuracy of charge measurement, Benner [20] used an electrostatic ion trap to recirculate ions through the conductive detection cylinder, which reduced the charge uncertainty to $2.3 e$ for an ion trapped for 450 passes. Dugourd and co-workers [21–24] used an ion-trapping CDMS instrument based on the design of Benner to obtain the mass and charge of polyethylene glycol (PEG) and DNA precursor ions in single-ion photodissociation experiments. Multiple detection electrodes have been incorporated into CDMS traps to improve signal averaging by increasing the number of measurements on each pass between the trapping electrodes and have been used to measure the mass distributions of synthetic polymers and nanoparticles as large as ~ 300 MDa [25]. In lieu of direct velocity measurements, Contino and Jarrold [26] demonstrated that the frequency of the periodic signal generated by a trapped ion measured using a Fourier transform (FT) can be used to determine the m/z of the ion and the amplitude measured at that frequency can be used to determine the charge of the ion. Using this technique, Jarrold and co-workers [27–34] have investigated pyruvate kinase multimers with masses ranging from 0.25 to 1.5 MDa and the assembly mechanisms of several viruses with masses ranging from 2 to 50 MDa.

The overall uncertainty in mass measurement in CDMS depends on the uncertainty in both the charge and m/z measurement. Uncertainty in the charge measurement can be reduced significantly by trapping the ion for longer times. By cryogenically cooling their detection electronics, optimizing CDMS instrumentation for longer ion trapping times and using improved FT analysis techniques, Jarrold and co-workers [26, 35, 36] have significantly improved the limits of detection ($\sim 7 e$) and the precision of charge measurement in ion-trapping CDMS, with uncertainties as low as $0.196 e$ rmsd for ions trapped for 3 s. With this substantial reduction to charge uncertainties measured for ions using CDMS, uncertainty in ion mass is largely determined by the uncertainty in m/z [36]. The distribution of ion energy per charge (eV/z) admitted into the CDMS trap currently limits this m/z uncertainty [35, 37]. A dual hemispherical deflection analyzer [26] (0.6% eV/z full width at half maximum (FWHM)) and turning quadrupole [38] (2% eV/z FWHM) have both been utilized to decrease the width of the initial ion energy distribution prior to trapping.

More recent work on CDMS instrumentation and analysis has shown that the oscillation frequency and energy per charge of an ion gradually change over the course of the trapping period, which can significantly increase the uncertainty in m/z measurements [37–39]. This change is a result of collisions with background gas and, for larger ions, solvent evaporation from the intact ion that occurs during the early stages of the trapping period. Both of these effects result in decreased ion energy per charge and increased ion oscillation frequency [38, 39]. Ion fragmentation, in contrast, can yield large, sudden changes in the energy per charge of the ion and ion oscillation frequency [38, 39]. Keifer et al. [39] observed that hepatitis B virus capsids (~ 4 MDa) gradually increased in frequency and primarily attributed this effect to solvent mass loss. They also observed sudden jumps in ion frequency corresponding to loss of 1 kDa that they attributed to solvated ion loss. Elliott et al. [38] quantified a relationship between the ion energy per charge and the turning-time ratio (TTR), the ratio of the time required for an ion to turn around in the trapping potential, and the time required to pass through the detection cylinder, measured from the separation between pulses in the time domain signal. Using this relationship, ion energy per charge was determined for each 10-ms segment of a PEG ion trapped for 4 s, enabling the accurate determination of the ion mass in each 10-ms segment even after six fragmentation events, solvent evaporation, and background collisions drastically changed the ion energy per charge from its initial value. Because the energy of each fragment ion can be measured, the masses of each fragment ion can be obtained as well [38]. With this method, MS^7 measurements of a single ion initially trapped in a CDMS instrument have been demonstrated [38]. The energy lost to background collisions for the precursor ion and the final fragment ion was also measured and used to gain information about the collision cross sections of these ions [38]. This method to measure ion energies via their TTR requires that the signal be higher than the noise in the time domain signal ($\sim 300 e$) [38]. An alternative method was introduced to measure the collision induced decrease in energy per charge of protein ions trapped in a CDMS instrument with masses ranging from 8.6 to 66.5 kDa and charges from $+8$ to $+53$ [37]. This energy measurement method uses a relationship between frequency change and ion energy per charge that requires that the analyte ion m/z be known, which, in turn, requires resolved charge states in the mass histogram. The total energy losses measured for these protein ions correlate well with collision cross sections measured using drift ion mobility [37]. This indicates that measurements of the time evolution of energy per charge of single ions can provide information about ion shape similar to that gained using conventional ion mobility techniques despite the significant differences in these methods.

In this work, a method using the higher-order harmonics of the FT of the CDMS ion signal to determine ion energy per charge is demonstrated. This method does not require that the analyte ion have sufficient charge to produce signal above the noise level in the time domain, and it does not require the ion to have a known m/z , making this method more universally

applicable than previous methods [37, 38] used for ion energy determination. The unconstrained nature of this ion energy measurement largely precludes the need for ion energy selection prior to the trapping and analyzing the masses of individual ions. Because this ion energy measurement is made dynamically in situ, the change in energy over time can be monitored to gain ion cross sections, mass changes due to solvent evaporation, and mass changes due to molecular fragmentation.

Experimental

Experiments were performed using a home-built charge detection mass spectrometer that has been described in detail previously [38]. Briefly, ions are formed by nanoelectrospray ionization using borosilicate capillaries and enter the instrument through a modified Z-Spray source (Waters, Milford, MA, USA). Ions then travel through two RF-only quadrupole ion guides and an energy-selective turning quadrupole (Ardara Technologies, Ardara, PA, USA). The turning quadrupole directs the energy-selected ions into the electrostatic cone trap that contains the detection cylinder. The pressure in the vacuum chamber housing the electrostatic cone trap is approximately 5×10^{-9} Torr. Polyethylene glycol (PEG) with a nominal molecular weight of 4 MDa was obtained from Sigma-Aldrich (St. Louis, MO, USA) and was prepared at a concentration of 120 nM in 50:50 water-methanol and used without further purification.

Ions induce a charge pulse when passing through the detection cylinder. These pulses are amplified by a CoolFET charge-sensitive preamplifier and a linear voltage amplifier (Amptek, Bedford, MA, USA). An additional shaping amplifier (Amptek, Bedford, MA, USA) is also used in a second detection channel and has been described previously [38]. PEG ions studied in this work have sufficient charge ($> 300 e$) that the signal of a single ion that passes through the detection cylinder one time is above the noise in the time domain signal recorded in the shaped channel, which is used to control the ion trap. The entrance of an ion into the detection cylinder triggers the raising of the potential of the front electrode of the trap to equal that of the back electrode for a specifiable time (500 ms in these experiments). The time domain signal generated by a trapped, oscillating ion is analyzed offline by a LabVIEW program described previously [25] that finds peaks of consistent size and spacing in the signal from the shaped channel. Data from ions trapped for less than 5 ms were discarded. All FT analysis is performed using the unshaped channel, with another LabVIEW program that performs a 5-ms segmented FT and records the amplitudes of both the fundamental and second harmonic peaks as well as the ion frequency for each segment. With the minimum trapping time set to 5 ms, the average trapping time for the ions measured here was 254 ms, with 21% of ions trapped for the 500-ms maximum trapping time.

Results and Discussion

Individual Ion Energies from Ratio of Harmonic Amplitudes

In CDMS, analyte ions pass through a detection tube and the charge pulse induced by the ion is measured. In trapped ion FT-CDMS, ions are recirculated through the detection tube inside an electrostatic trap, producing a regular series of pulses well suited to analysis by FT. The relative amplitudes of the fundamental frequency and harmonic frequencies in a FT of a pulse train depends on the pulse shape and duty cycle of the periodic signal. CDMS signals resemble an ideal pulse train, where the time spent by an ion inside the tube is the “on” portion of the cycle and the time spent outside the tube is “off.” For signals with the shape of an ideal pulse train, the relationship between the FT amplitude of the n th harmonic frequency, a_n , the time domain amplitude (A), and the duty cycle (d) is given by Eq. 1 [40].

$$a_n = \frac{2A}{n\pi} \sin(n\pi d) \quad (1)$$

The time domain signals for two ideal pulse trains of the same frequency with duty cycles of 0.3 and 0.4 are shown in Fig. 1 along with the corresponding harmonic frequency amplitudes obtained from the FT of the time domain signals. The two pulse trains have markedly different distributions of amplitude among the harmonic frequencies that result from the different duty cycles. Because specific distributions of harmonic intensities correspond to specific duty cycles, they can be used as a “fingerprint” that characterizes the duty cycle in the time domain signal.

The ratio of the amplitudes of any two harmonic frequencies can be calculated from Eq. 1. This ratio does not depend on the time domain amplitude, A . The equation for the ratio of the first and second harmonics is a special case that can be simplified significantly and is given by Eq. 2.

$$\frac{a_1}{a_2} = \sec(\pi d) \quad (2)$$

This equation for the ratio of the first two harmonic amplitudes is one illustration of the fundamental relationship between the ratio of any two harmonic amplitudes in the FT of a pulse train and its duty cycle. Hereafter, the ratio of a_1 and a_2 given by Eq. 2 will be used exclusively and will be referred to as the harmonic amplitude ratio (HAR). Any other ratio of harmonic frequency amplitudes can also be mathematically related to the duty cycle. However, the first and second are the two largest harmonics for duty cycles observed in the CDMS instrument used here, so defining the HAR with these peaks maximizes the signal-to-noise ratio (S/N) for determining these values from experimental data.

The pulse train produced by an ion trapped in a CDMS instrument has been characterized using the TTR, which is the ratio of the time an ion spends outside the detection cylinder to

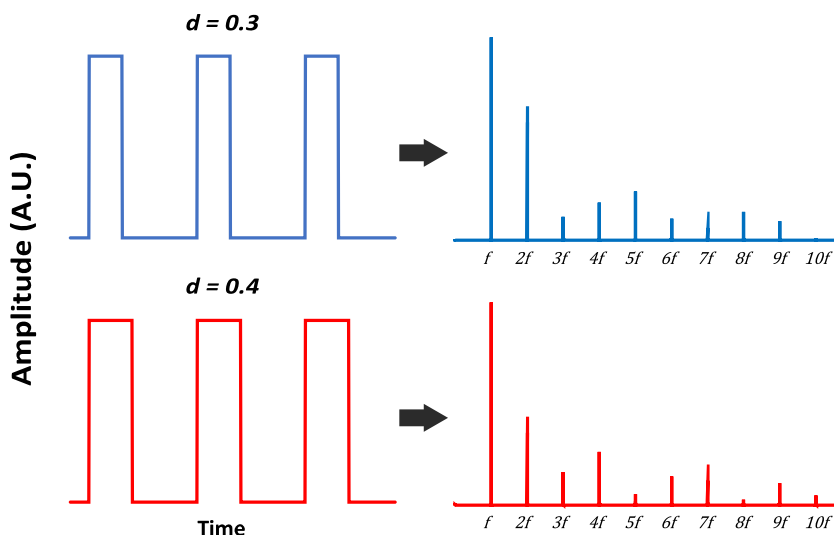


Figure 1. Ideal pulse trains (left) with duty cycles of 0.4 (top) and 0.3 (bottom) and the corresponding FT harmonic amplitudes (right). Small differences in the duty cycle result in significantly different harmonic amplitude distributions

the time spent inside the detection cylinder [38]. The duty cycle is related to the TTR, and appropriate substitution in Eq. 2 yields a relationship between HAR and TTR for an ideal pulse train that is given by Eq. 3.

$$\text{HAR} = \sec\left(\frac{\pi}{\text{TTR} + 1}\right) \quad (3)$$

The relationship between the TTR and the energy per charge for a single ion, including the effects of ions injected off-axis and at angles resulting in off-center axis trajectories, has been characterized previously using SIMION ion trajectory simulations for the trap geometry employed here and a trap potential of 330 V [38]. In this study, SIMION simulations were performed over a range of trap potentials from 100 to 500 V on ions traveling along the longitudinal trap axis to characterize the ion energy per charge/TTR relationship over a broader set of instrumental conditions. The relationship between ion energy per charge and TTR depends on the trap potential, but the ratio of the trap potential to the ion energy per charge yields a constant TTR value. Thus, the ion energy per charge can be determined for any ion from the applied trap potential and the measured TTR. This result makes ion energy selection prior to the trap unnecessary for accurate single ion mass measurements because the energy per charge of each ion can be measured dynamically in situ. Further information about the SIMION simulations is provided in the [Supporting Information](#).

For the ion trap geometry used here, the stable range of ion TTRs is ~ 1.7 – 2.4 , over which Eq. 3 is continuous. For different trap geometries with a stable TTR range where Eq. 3 is not continuous, a different set of harmonic frequency amplitudes could be used. Thus, for a known trap geometry, the HAR measured in the FT can be directly related to the energy per charge of an unknown ion. A previous method used to determine ion energy per charge required that the signal induced by an ion is above the noise in the time domain [38]. This

requirement for an observable signal directly in the time domain spectrum restricts this prior method to large ions that have sufficient charge (~ 300 charges) [38]. An advantage of this new method, in which the ion energy is obtained from the HAR, is that it does not require that the time domain signal induced by a single ion produce an observable signal above the noise but rather only that the first and second harmonic be observable in the FT of the signal. This makes it possible to apply this method to smaller ions with many fewer charges. Another method demonstrated previously makes it possible to determine ion energies for low charge ions, but this method requires known ion m/z values obtained from resolved charge states of proteins with known mass [37]. The HAR measurement can be used to determine the energy per charge of ions without any prior knowledge of the ion m/z and charge state, making this method more generally applicable to ions of any size or charge.

Ion Signal Simulation

The dimensions of the ion trap, the ion velocity, and the RC time constant associated with the electronic components of the detector can affect the shape and amplitude of the pulse train generated by a trapped ion. In this work, a SIMION simulation similar to that performed by Alexander et al. [41] was used to simulate the shape of the pulse induced by an ion passing through a cylindrical detection tube with the same dimensions and surroundings used in the experiments. This pulse shape was then appropriately scaled by the simulated ion velocity derived from a specified frequency and TTR. A simulated pulse train 25 ms in length was generated by concatenating copies of the pulse shape at the simulated ion frequency then sampled at 5 MHz, which was chosen to match the sampling rate typically used in these CDMS experiments. Finally, a simulated RC constant of 20 μs was applied across the entire transient using an iterative method described by Weinheimer [42]. A RC constant of 20 μs was determined from the decay of the output

signal after charge pulses were applied to the detection circuit of the CDMS instrument used here. The FT of these simulated pulse trains was then used to calculate the HAR.

A single pulse of this simulated signal is compared to an ideal pulse of the same duration in Fig. 2 (inset). The significantly different pulse shape compared to an ideal waveform results in small perturbations to the harmonic amplitudes in the FT described by Eq. 1. As a result, the relationship between HAR and TTR is also affected. To quantify this effect, simulated ion signals were generated at intervals of 0.05 TTR over the range of TTRs that are stable in the CDMS ion trap used here (1.70–2.40 TTR) and at a frequency of 40 kHz. The HARs measured for the simulated signals were compared to the calculated HARs of ideal pulse trains over the same range of TTR. The HAR values for the simulated ion signal are slightly greater than those of the ideal pulse train (Fig. 2). Because the perturbed mathematical relationship between TTR and HAR for the simulated ion signal is not straightforward to derive, a 3rd-order polynomial fit was instead used to model the data and is given in Eq. 4.

$$\text{HAR} = -1.1653 \times \text{TTR}^3 + 8.3686 \times \text{TTR}^2 - 20.724 \times \text{TTR} + 19.309 \quad (4)$$

Although the functional form of this fit may not be appropriate for extrapolation outside the range of TTR simulated (1.7–2.4), the R^2 value (0.99996) indicates an excellent fit within this range.

Comparison of Model to Signals of PEG Ions

To validate this model for the signals of trapped ions, the TTR predicted using the HAR of real ion signal must be compared to an independent measurement of TTR. The TTR can be readily obtained from analysis of the data as long as ions have enough charge to produce a signal above the noise in the time domain signal [38]. Obtaining the TTR this way provides a reasonably accurate measurement of energy per charge, with an uncertainty of $\sim 1\%$ that mainly originates from ions that have trajectories that are slightly off-center [38].

In this work, the TTR was measured using this time-domain method for 3538 segments of PEG ion signal 5 ms in length taken from 82 individual PEG ions. The HAR measured in the FT of each 5-ms segment was also recorded. Although ions that have a broad range of frequencies were detected, only segments with an average frequency between 39.5 and 40.5 kHz were included in this analysis in order to match the simulated ion signal frequency of 40 kHz. The shape of the waveform does depend slightly on frequency. However, the relationship between HAR and TTR at a single frequency is sufficient to illustrate this method. A 5-ms FT segment length was chosen to minimize broadening of the FT peaks owing to the slow frequency shift that occurs because of ion collisions with background gas. This broadening attenuates higher-order harmonics disproportionately more than the fundamental

frequency, leading to inflated HAR values. This effect constrains the length of the time segment that can be transformed and used to obtain accurate ion TTR values. However, the same effect means that HAR values are also sensitive to sudden changes in ion oscillation frequency that have been observed previously [37, 38]. These sudden changes in ion frequency, caused by ion trajectory instability or fragmentation, can broaden or even split the FT peak for a single ion within a 5-ms segment, resulting in artificially lowered amplitudes and anomalously high values of the HAR. To filter out these errant data points, the HARs measured for each 5-ms segment of a single ion signal are fit using a bisquare linear regression that iteratively reduces the weight of outliers in a least squares regression. Segments with a HAR value more than three standard deviations away from the fit value are discarded. This process is reiterated with the remaining HAR values until there are no outliers; for the ions studied here, $\sim 6\%$ of segments were discarded by this procedure.

PEG ions with a wide range of TTR values (~ 1.8 –2.4) near the selected 40-kHz oscillation frequency were generated by broadening the energy range of the PEG ions admitted to the trap by the turning quadrupole to be similar in width to the energy distribution produced in the ion source. Different ion source conditions were used to produce different distributions of ion energy that cover the range investigated here. Ion segments were binned in increments of 0.01 TTR, and the mean HAR values are plotted in Fig. 3 for bins containing more than 20 ion segments. The bin size of 0.01 TTR closely approximates the average uncertainty in the time domain measurement of the TTR of ions at 40 kHz. The error bars shown represent one standard deviation in the distribution of HAR of ions within each bin. The simulated signal fit given by Eq. 4 is also shown and matches well with the trend observed for the real ion signals. The gap in the experimental data from 1.95 to 2.00 TTR is not due to an uneven sampling of PEG ion energies; ions in this range are unstable and are quickly lost from the trap. A possible explanation for this observation is an imperfection in the experimental potential surface that results in unstable trajectories at the ion energies represented by this range of TTR. The mean deviation from the fit is $+0.6\%$, and the standard deviation for all the individual 5-ms segments is 1.7% . The mean deviation is much lower than the statistical spread of the data due to noise in the experimental data. The positive mean deviation observed may be due to the small frequency shift caused by collisions with background gas that occur during the 5-ms data segments. This frequency shift disproportionately broadens the different harmonic peaks in the FT, leading to a slightly increased HAR value. Overall, this analysis indicates that using the simulated signal fit for HAR is a good model for the experimental signal. Importantly, it demonstrates that the TTR and, by extension, the energy per charge of an ion can be measured directly and accurately using the HAR alone.

This new method of using the HAR to obtain TTR values results in slightly higher standard deviation in the TTR measured for each 5-ms segment of a trapped ion (1.7%) compared

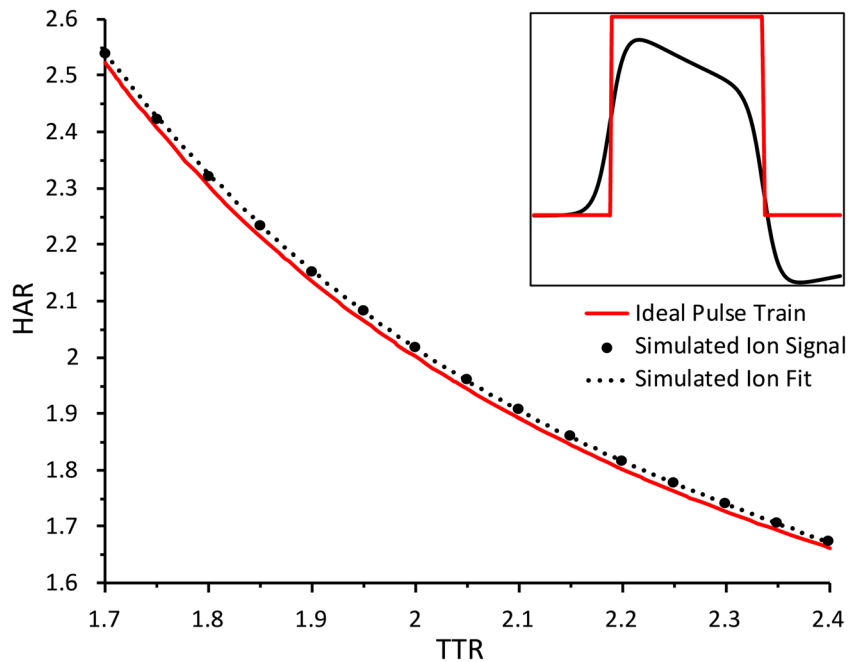


Figure 2. Comparison of the dependence of HAR on TTR for an ideal pulse train (red) and simulated ion pulse train (black). The difference in pulse shape (inset) results in consistently higher values of the HAR for the simulated signal. The HAR values of the simulated signal are fit with a 3rd-order polynomial (dotted line)

to inherent uncertainty in the TTR-energy calibration owing to different possible ion trajectories ($\sim 1\%$), but this limitation can largely be overcome by taking advantage of long total trapping times for ions. Figure 4 shows a plot of the energy per charge measured using the HAR at each of the 5-ms segments for two

PEG ions trapped for 500 ms. The charges measured for ion no. 1, shown in red, and ion no. 2, shown in black, are 893 ± 1 and 1262 ± 1 charges, respectively, and do not change significantly during the trapping period. The energy per charge for both ions decreases with time. This decrease in the energy per charge of

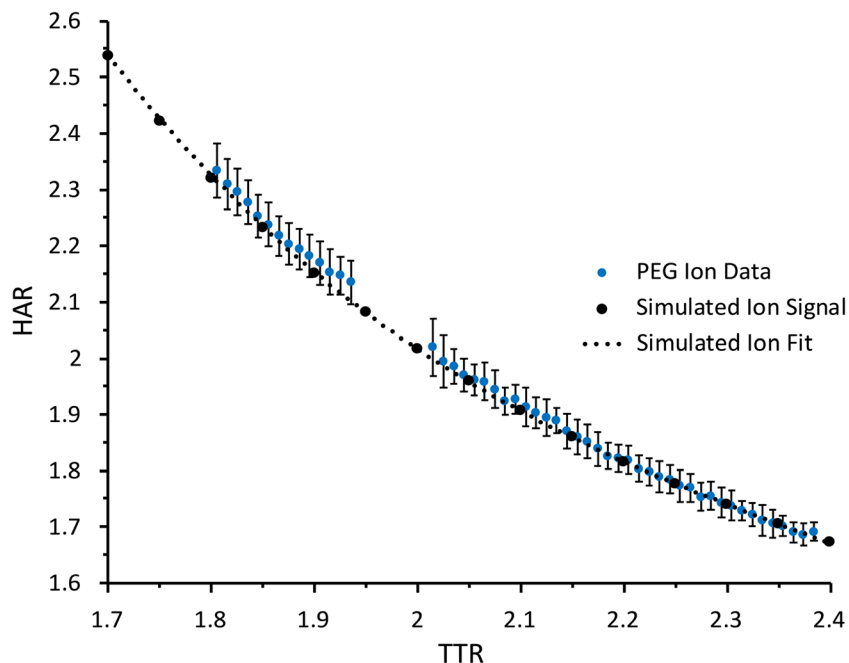


Figure 3. Comparison of the simulated signal HAR dependence on TTR to values measured for 5-ms segments of the PEG ion signal. For the PEG ions, TTR was measured independently of the HAR. Error bars indicate one standard deviation of the values measured for PEG ions binned in increments of 0.01 TTR. The 0.01 TTR bin size roughly corresponds to the average uncertainty in the time domain TTR measurements for ions at 40 kHz. The gap in PEG ion data from 1.95 to 2.00 TTR is not due to uneven sampling. Ions in this range are unstable and are lost quickly from the trap, perhaps due to imperfections in the experimental trapping potential

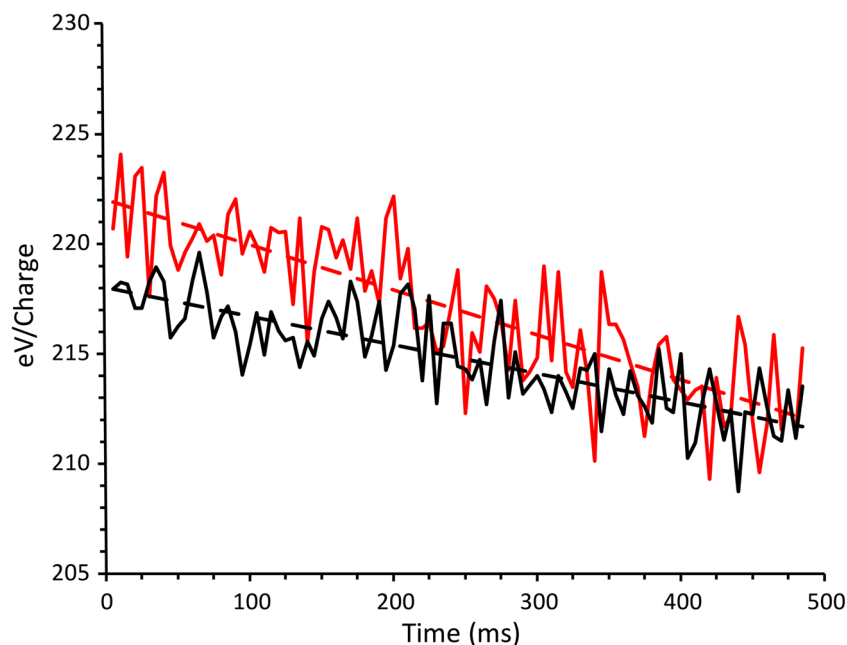


Figure 4. Energy per charge measured using HAR for each 5-ms signal segment of PEG ions trapped for 500 ms data from ion no. 1 (red) and ion no. 2 (black) were fit using a linear regression (dotted lines). Ion 1 has larger energy per charge loss than ion 2 over the same length of time, indicating a greater extent of mass loss and a less dense structure

the ions is consistent with previous results for single small protein ions [37] and PEG ions [38] where energy loss was measured using known ion m/z or time domain analysis, respectively. These decreases in ion energy per charge can be fit using a linear regression (shown in Fig. 4) with slopes of -0.021 and -0.013 eV/z-ms, intercepts of 220.4 and 216.9 eV/z, and standard errors of 1.9 and 1.4 eV/z for ion no. 1 and no. 2, respectively. Using these intercept energies and the initial ion frequencies (39.406 and 39.423 kHz, respectively), the initial m/z 's were determined to be 3544 ± 31 and 3602 ± 24 Da/z, for ions no. 1 and no. 2, respectively. From the independent m/z and charge measurements, the initial masses of these two ions were determined to be 3.15 ± 0.03 and 4.54 ± 0.03 MDa, respectively. The final masses measured for these ions, obtained from the ion energy per charge determined from each fit at 500 ms, were 2.99 ± 0.02 and 4.39 ± 0.02 MDa. Thus, these ions lost 0.16 ± 0.04 and 0.15 ± 0.03 MDa during the time that they were trapped, consistent with solvent evaporation from these ions [38].

The standard deviation of the fit in energy per charge is 0.88 and 0.63%, respectively, of the initial energy of each ion. This is significantly lower than the 1.7% uncertainty associated with each individual 5-ms segment because many 5-ms segments are used to obtain these values. Because neither the time domain or HAR method for obtaining ion energies accounts for the $\sim 1\%$ uncertainty associated with off-center trajectories, any error in the fit that is below 1%, as is the case for these PEG ion energies measured using HAR, is no longer the dominant limitation in obtaining accurate ion energies. For lower charge analytes that induce smaller signals and have correspondingly higher relative uncertainties in the amplitudes measured for each harmonic, the standard uncertainty in these measurements can be decreased by using longer ion trapping times, although a more sophisticated

fitting function may be necessary to accurately reflect the change in the TTR over time. Jarrold et al. [39] used an exponential function to model ion energy loss in CDMS over a 3-s time period. However, the relatively small percentage of energy loss and much shorter 500-ms ion trapping time used justify the simpler linear regression fits used here.

Ion Cross Sections from Energy Loss Measurements

Measuring the energy per charge of each ion directly as a function of time has several advantages in CDMS measurements. Accurate ion energy measurements in CDMS can be used to increase the accuracy of mass measurements when ions with a relatively broad range of energies are introduced into the trap making it possible to increase the ion throughput for dilute samples where few ions are formed. Mass losses due to fragmentation events and solvent evaporation can change ion energies during a trapping period; measurements of ion energy make it possible to quantify these mass changes. Ion energy measurements also have the potential to provide information about the cross sections of individual ions that are weighed in the trap. For previous work on small protein ions ranging from 8 to 65 kDa, the total ion energy loss over a 500-ms period was shown to be linearly correlated with the collision cross sections measured using more conventional ion mobility measurements on ensembles of ions, suggesting that ion energy loss can be used to obtain a measure of the collision cross section of each individual ion in CDMS [37].

The total energy loss was determined for the PEG ions studied here by taking the difference of the energy per charge fit at 0 and 500 ms and multiplying by the total charge; ion no. 1 lost 8.7 keV and ion no. 2 lost 7.8 keV over the course of the trapping period. These total energy losses are the sum of two

energy loss mechanisms: collisions with background gas that reduce ion kinetic energy and solvent evaporation that changes the ion mass. Previous work using a SIMION simulation of an ion that lost a constant mass per unit time but experienced no collisions with background gas demonstrated that these two mechanisms for energy loss can be deconvolved [38]. Using additional SIMION simulations, this method has been generalized by determining the relationship between the percentage of mass lost and the percentage energy lost by ions with a range of TTRs that span the stable range of the current trap geometry (1.7–2.4). Ions with a higher TTR lose more energy for the same relative mass loss than ions at lower TTR. Additional detail on these SIMION simulations is provided in the [Supporting Information](#).

For the PEG ions studied here, mass losses account for 6.4 and 5.7 keV of the total energy lost for each ion, respectively. The remaining 2.3 and 2.1 keV of energy lost from each ion is due to collisions with background gas. Extrapolation of the linear correlation between ion energy and collision cross section observed previously [37] yields cross section values of 1150 and 1060 nm² for ions 1 and 2, respectively. Uetrecht et al. [43] previously determined collision cross sections of 680–710 and 870–910 nm² for hepatitis B virus (HBV) capsid conformers weighing 3.01 and 4.02 MDa ($T=3$ and $T=4$ capsids, respectively). These cross section values are lower than those of the PEGs of similar mass measured here, but the differing charge and structure of the HBV ion is consistent with this difference. The HBV ions measured had average charges of 140 and 160 for the $T=3$ and $T=4$, capsids, respectively, and exhibit compact icosahedral structures [43]. In contrast, the PEG ions measured here have 893 and 1262 charges and, as a single chain polymer, a much less compact structure is expected. Both effects could contribute to a more disorganized, less compact structure that yields the higher cross section values observed. It is also important to note that the absolute accuracy of the cross section values determined for PEG is almost certainly limited by extrapolating a trend observed previously for much smaller ions. However, the relative cross sections determined by collisional energy loss are limited only by the precision of the energy and charge values measured. Because of the larger cross section and smaller mass observed for ion no. 1, we conclude that ion no. 1 is much less dense than ion no. 2, indicating that the shapes of the two ions are significantly different. Additional experiments are underway to improve the cross section calibration by measuring CDMS energy losses for large molecules and macromolecular complexes for which accurate cross section values have been determined using more conventional ion mobility techniques. However, these results demonstrate that the new CDMS methods developed here make it possible to simultaneously measure the mass, charge, and cross section of individual ions of virtually any size.

Conclusions

A fundamental relationship between the TTR of the pulse train produced by an ion trapped in a CDMS instrument and the

corresponding FT harmonic amplitudes makes it possible to measure the ion energy using only the FT of the ion signal. Simulated ion signals accounting for nonideal pulse train characteristics are used to calibrate the relationship between the HAR and TTR. The validity of this calibration is confirmed by comparison to PEG ions for which the TTR is measured using a method independent from the measured HAR. The mean deviation between the TTR determined for each 5-ms segment of PEG signal using the HAR and the independent TTR measurement is 0.6%, much less than the $\sim 1\%$ uncertainty [38] in converting TTR measurements to ion energies that stems from the range of possible ion trajectories within the trap.

The energy per charge of two PEG ions trapped for 500 ms is monitored using the HAR over their respective trapping times. A fit of these values over time decreases the uncertainty associated with both the initial energy and mass measurement. Both ions show significant decreases in energy per charge over time due to solvent evaporation and collisions with background gas. Notably, the PEG ion with lower initial mass (3.15 MDa) loses more total energy than the higher initial mass ion (4.54 MDa). Combined with the greater mass loss for the smaller ion, this disproportional loss of energy suggests that the low mass PEG ion exhibits a less dense gas phase conformation than the high mass ion. This observation also demonstrates that energies determined using HARs can be used to gain information about single ion cross sections. Because this FT harmonic analysis does not require a known ion m/z or ion signal observable above the time-domain noise, it can be applied to determine the mass and cross sections of ions that were previously inaccessible using CDMS techniques or conventional ion mobility/mass spectrometry. Current work is underway to extend the relationship between energy loss and collisional cross section to higher masses, using large molecules for which accurate collisional cross sections have been measured with more conventional ion mobility instruments.

Acknowledgements

This material is based upon work supported by the National Science Foundation under CHE-1609866. The authors thank Professor Martin F. Jarrold for helpful discussions and Professor Ryan R. Julian for his innovative contributions to science.

References

1. Snijder, J., Rose, R.J., Veessler, D., Johnson, J.E., Heck, A.J.: Studying 18 MDa virus assemblies with native mass spectrometry. *Angew. Chem. Int. Ed.* **52**, 4020–4023 (2013)
2. Lössl, P., Snijder, J., Heck, A.J.R.: Boundaries of mass resolution in native mass spectrometry. *J. Am. Soc. Mass Spectrom.* **25**, 906–917 (2014)
3. Smith, R.D., Cheng, X., Brace, J.E., Hofstadler, S.A., Anderson, G.A.: Trapping, detection and reaction of very large single molecular ions by mass spectrometry. *Nature.* **369**, 137–139 (1994)
4. Bruce, J.E., Cheng, X., Bakhtiar, R., Wu, Q., Hofstadler, S.A., Anderson, G.A., Smith, R.D.: Trapping, detection, and mass measurement of individual ions in a Fourier transform ion cyclotron resonance mass spectrometer. *J. Am. Chem. Soc.* **116**, 7839–7847 (1994)

5. Wuerker, R.F., Shelton, H., Langmuir, R.V.: Electrodynamic containment of charged particles. *J. Appl. Phys.* **30**, 342–349 (1959)
6. Philip, M.A., Gelbard, F., Arnold, S.: An absolute method for aerosol particle mass and charge measurement. *J. Colloid Interface Sci.* **91**, 507–515 (1983)
7. Hars, G., Tass, Z.: Application of quadrupole ion trap for the accurate mass determination of submicron size charged particles. *J. Appl. Phys.* **77**, 4245–4250 (1995)
8. Schlemmer, S., Illema, J., Wellert, S., Gerlich, D.: Nondestructive high-resolution and absolute mass determination of single charged particles in a three-dimensional quadrupole trap. *J. Appl. Phys.* **90**, 5410–5418 (2001)
9. Nie, Z., Tzeng, Y., Chang, H., Chiu, C., Chang, C., Chang, C., Tao, M.: Microscopy-based mass measurement of a single whole virus in a cylindrical ion trap. *Angew. Chem. Int. Ed.* **45**, 8131–8134 (2006)
10. Cai, Y., Peng, W.P., Kuo, S.J., Lee, Y.T., Chang, H.C.: Single-particle mass spectrometry of polystyrene microspheres and diamond nanocrystals. *Anal. Chem.* **74**, 232–238 (2002)
11. Shelton, H., Hendricks, C.D., Wuerker, R.F.: Electrostatic acceleration of microparticles to hypervelocities. *J. Appl. Phys.* **31**, 1243–1246 (1960)
12. Hendricks Jr., C. D.: Charged droplet experiments. *J. Colloid Sci.* **17**, 249–259 (1962)
13. Stradling, G. L., Idzorek G. C., Shafer B. P., Curling Jr. H. L., Collopy M. T., Blossom A. A. H., Fuerstenau S.: Ultra-high velocity impacts: cratering studies of microscopic impacts from 3 km/s to 30 km/s. *Int. J. Impact. Eng.* **14**, 719–727 (1993)
14. Viodé, A., Dagany, X., Kerleroux, M., Dugourd, P., Doussineau, T., Charles, L., Antoine, R.: Coupling of size-exclusion chromatography with electrospray ionization charge-detection mass spectrometry for the characterization of synthetic polymers of ultra-high molar mass. *Rapid Commun. Mass Spectrom.* **30**, 132–136 (2016)
15. Fuerstenau, S.D., Benner, W.H., Thomas, J.J., Brugidou, C., Bothner, B., Siuzdak, G.: Mass spectrometry of an intact virus. *Angew. Chem. Int. Ed.* **40**, 542–544 (2001)
16. Fuerstenau, S.D., Benner, W.H.: Molecular weight determination of Megadalton DNA electrospray ions using charge detection time-of-flight mass spectrometry. *Rapid Commun. Mass Spectrom.* **9**, 1528–1538 (1995)
17. Schultz, J.C., Hack, C.A., Benner, W.H.: Mass determination of Megadalton-DNA electrospray ions using charge detection mass spectrometry. *J. Am. Soc. Mass Spectrom.* **9**, 305–313 (1998)
18. Doussineau, T., Désert, A., Lambert, O., Taveau, J., Lansalot, M., Dugourd, P., Bourgeat-Lami, E., Ravaine, S., Duguet, E., Antoine, R.: Charge detection mass spectrometry for the characterization of mass and surface area of composite nanoparticles. *J. Phys. Chem. C.* **119**, 10844–10849 (2015)
19. Doussineau, T., Bao, C.Y., Antoine, R., Dugourd, P., Zhang, W., D'Agosto, F., Charleux, B.: Direct molar mass determination of self-assembled amphiphilic block copolymer nanoobjects using electrospray-charge detection mass spectrometry. *ACS Macro Lett.* **1**, 414–417 (2012)
20. Benner, W.H.: A gated electrostatic ion trap to repetitiously measure the charge and *M/Z* of large electrospray ions. *Anal. Chem.* **69**, 4162–4168 (1997)
21. Doussineau, T., Yu Bao, C., Clavier, C., Dagany, X., Kerleroux, M., Antoine, R., Dugourd, P.: Infrared multiphoton dissociation tandem charge detection-mass spectrometry of single Megadalton electrosprayed ions. *Rev. Sci. Instrum.* **82**, 084104 (2011)
22. Doussineau, T., Antoine, R., Santacreu, M., Dugourd, P.: Pushing the limit of infrared multiphoton dissociation to Megadalton-size DNA ions. *J. Phys. Chem. Lett.* **3**, 2141–2145 (2012)
23. Antoine, R., Doussineau, T., Dugourd, P., Calvo, F.: Multiphoton dissociation of macromolecular ions at the single-molecule level. *Phys. Rev. A.* **87**, 013435 (2013)
24. Doussineau, T., Paletto, P., Dugourd, P., Antoine, R.: Multiphoton dissociation of electrosprayed Megadalton-sized DNA ions in a charge-detection mass spectrometer. *J. Am. Soc. Mass Spectrom.* **26**, 7–13 (2015)
25. Elliott, A.G., Merenbloom, S.I., Chakrabarty, S., Williams, E.R.: Single particle analyzer of mass: a charge detection mass spectrometer with a multi-detector electrostatic ion trap. *Int. J. Mass Spectrom.* **414**, 45–55 (2017)
26. Contino, N.C., Jarrold, M.F.: Charge detection mass spectrometry for single ions with a limit of detection of 30 charges. *Int. J. Mass Spectrom.* **345–347**, 153–159 (2013)
27. Pierson, E.E., Keifer, D.Z., Contino, N.C., Jarrold, M.F.: Probing higher order multimers of pyruvate kinase with charge detection mass spectrometry. *Int. J. Mass Spectrom.* **337**, 50–56 (2013)
28. Pierson, E.E., Keifer, D.Z., Selzer, L., Lee, L.S., Contino, N.C., Wang, J.C., Zlotnick, A., Jarrold, M.F.: Detection of late intermediates in virus capsid assembly by charge detection mass spectrometry. *J. Am. Chem. Soc.* **136**, 3536–3541 (2014)
29. Keifer, D.Z., Pierson, E.E., Hogan, J.A., Bedwell, G.J., Prevelige, P.E., Jarrold, M.F.: Charge detection mass spectrometry of bacteriophage P22 Procapsid distributions above 20 MDa. *Rapid Commun. Mass Spectrom.* **28**, 483–488 (2014)
30. Kukreja, A.A., Wang, J.C., Pierson, E., Keifer, D.Z., Selzer, L., Tan, Z., Dragnea, B., Jarrold, M.F., Zlotnick, A.: Structurally similar woodchuck and human hepadnavirus core proteins have distinctly different temperature dependences of assembly. *J. Virol.* **88**, 14105–14115 (2014)
31. Pierson, E.E., Keifer, D.Z., Kukreja, A.A., Wang, J.C., Zlotnick, A., Jarrold, M.F.: Charge detection mass spectrometry identifies preferred non-icosahedral polymorphs in the self-assembly of woodchuck hepatitis virus capsids. *J. Mol. Biol.* **428**, 292–300 (2016)
32. Pierson, E.E., Keifer, D.Z., Asokan, A., Jarrold, M.F.: Resolving adeno-associated viral particle diversity with charge detection mass spectrometry. *Anal. Chem.* **88**, 6718–6725 (2016)
33. Keifer, D.Z., Motwani, T., Teschke, C.M., Jarrold, M.F.: Acquiring structural information on virus particles with charge detection mass spectrometry. *J. Am. Soc. Mass Spectrom.* **27**, 1028–1036 (2016)
34. Lutowski, C.A., Lykтей, N.A., Zhao, Z., Pierson, E.E., Zlotnick, A., Jarrold, M.F.: Hepatitis B virus capsid completion occurs through error correction. *J. Am. Chem. Soc.* **139**, 16932–16938 (2017)
35. Pierson, E.E., Contino, N.C., Keifer, D.Z., Jarrold, M.F.: Charge detection mass spectrometry for single ions with an uncertainty in the charge measurement of 0.65 e. *J. Am. Soc. Mass Spectrom.* **26**, 1213–1220 (2015)
36. Keifer, D.Z., Shinholt, D.L., Jarrold, M.F.: Charge detection mass spectrometry with almost perfect charge accuracy. *Anal. Chem.* **87**, 10330–10337 (2015)
37. Elliott, A.G., Harper, C.C., Lin, H.-W., Susa, A.C., Xia, Z., Williams, E.R.: Simultaneous measurements of mass and collisional cross-section of single ions with charge detection mass spectrometry. *Anal. Chem.* **89**, 7701–7708 (2017)
38. Elliott, A.G., Harper, C.C., Lin, H.-W., Williams, E.R.: Mass, mobility, and MS^N measurements of single ions using charge detection mass spectrometry. *Analyst.* **142**, 2760–2769 (2017)
39. Keifer, D.Z., Alexander, A.W., Jarrold, M.F.: Spontaneous mass and charge losses from single multi-Megadalton ions studied by charge detection mass spectrometry. *J. Am. Soc. Mass Spectrom.* **28**, 498–506 (2017)
40. Smith, S.W.: The scientist and engineer's guide to digital signal processing, 1st edn. California Technical Publ, Calif (1997)
41. Alexander, J.D., Graham, L., Calvert, C.R., Kelly, O., King, R.B., Williams, I.D., Greenwood, J.B.: Determination of absolute ion yields from a MALDI source through calibration of an image-charge detector. *Meas. Sci. Technol.* **21**, 045802 (2010)
42. Weinheimer, A.J.: The charge induced on a conducting cylinder by a point charge and its application to the measurement of charge on precipitation. *J. Atmos. Ocean. Technol.* **5**, 298–304 (1988)
43. Uetrecht, C., Versluis, C., Watts, N.R., Wingfield, P.T., Steven, A.C., Heck, A.J.R.: Stability and shape of hepatitis B virus capsids in vacuo. *Angew. Chem. Int. Ed.* **47**, 6247–6251 (2008)